Structural Stability of a Stiffened Aluminum Fuselage Panel Subjected to Combined Mechanical And Internal Pressure Loads

Marshall Rouse* **and Richard D. Young****

Mechanical and Durability Branch
NASA Langley Research Center
Hampton, VA 23681-2199

Ralph E. Gehrki†

Lockheed Martin
Hampton, VA

Abstract

Results from an experimental and analytical study of a curved stiffened aluminum panel subjected to combined mechanical and internal pressure loads are presented. The panel loading conditions were simulated using a D-box test fixture. Analytical buckling load results calculated from a finite element analysis are presented and compared to experimental results. Buckling results presented indicate that the buckling load of the fuselage panel is significantly influenced by internal pressure loading. The experimental results suggest that the stress distribution is uniform in the panel prior to buckling. Nonlinear finite element analysis results correlates well with experimental results up to buckling.

Introduction

The structural stability of aircraft fuselage structures subjected to combined loading conditions representative of actual flight conditions is an important consideration when designing aerospace structures. Since testing full-scale fuselage structures is expensive, curved panels representative of these structures are often evaluated to better understand the response of fuselage structures. A limited amount of data exists that describes the response of fuselage structures subjected to combined mechanical loads and internal pressure(1-3). Also, there is a need for better understanding of buckling of fuselage structures subjected to combined mechanical loads and internal pressure since the load interactions could be non-intuitive.

This paper presents experimental and analytical results that describe the structural response of a curved stiffened panel subjected to combined mechanical and internal pressure loads using a D-box test fixture. Experimental and analytical results are presented that describe the initial buckling of an aluminum panel subjected to combined axial and in-plane shear loads, with and without internal pressure.

Test Specimen Description

The aluminum test panel considered in the present study has fifteen stringers and four frames. A photograph of the aluminum test panel is shown in Figure 1(a). The overall dimensions of the panel are 115.91-in. length, 121.16-in. width and 122.26-in. radius. The the panel skin is made from three 0.063-in-thick 2024-T3 aluminum sheets mechanically fastened together. The left and right skin sections have a 60.12- and 38.66-in.-arc width, respectively. The center skin section has a 38.66-in.-arc width. The stringers are mechanically fastened to the panel skin. Also, an aluminum tear strip is bonded to the skin of the panel under the frames and stringers. A photograph describing local structural details of the panel is presented in Figure 1(b). The panel geometry and stiffener details are described in Figure 2. As shown in Figure 2(a), the panel frames are made from 7075-T6 aluminum Z sections and are spaced 23.58-in. apart. The stringers are made from

* Senior Aerospace Engineer, Mechanics and Durability Branch. Senior Member, AIAA.

** Senior Aerospace Engineer, Mechanics and Durability Branch. Member, AIAA

† Aerospace Engineer.

7075-T6 aluminum hat sections spaced 7.03-in. apart. The frames are mechanically fastened to the skin of the panel by aluminum shear clips and to the stringers by aluminum tension ties. The cross-sectional geometry of the stringer is shown in Figure 2(b), the frame geometry is shown in Figure 2(c), and the shear clip and tension tie geometry is shown in Figure 2(d) and 2(e), respectively. Typical material properties for the two aluminum alloys used to construct the panel are presented in Table 1. The panel was instrumented with strain gages to record the panel response based on the analysis results for different typical loading conditions.

Combined Loads Test Machine and D-Box Test Fixture

The combined loads test machine and D-box test fixture configurations are illustrated in Figure 3. The details of the combined loads test machine are summarized in Ref. 2. The D-box test fixture has been designed to ensure that appropriate boundary conditions are imposed on a curved panel to provide a stress state that is representative of a cylindrical shell. This requirement is particularly important when investigating the failure of a curved panel.

The D-box test fixture shown in Figure 4(a) was used to apply mechanical and internal pressure loads to the test panel. The small axial stiffness of the D-box test fixture allows a test panel to experience most of the applied axial load and minimizes the shift in the center-of-pressure of the assembly if the test panel buckles. The low axial stiffness of the D-box test fixture is the result of an assembly of curved I-beams with the cross-section shown in the inset. The I-beam sections are 8.0-inches deep and 15 of these sections are used to make the D-box test fixture. This D-box test fixture is designed to test curved panels with 60- to 130-inch radii and 20- to 22-inch frame spacings. The panels are attached to the D-box test fixture with the hinge fittings as indicated in Figure 4(b). A cross-section of the D-box test fixture is presented in Figure 4(b) that shows the details of the hinge fittings. Thirteen of these hinge fittings are provided between the I-beams for this purpose. When the D-box assembly is internally pressurized, the assembly expands in a manner that causes the hinge supports to move inward. This deformation will cause the test panel to bend in a way that is not representative of the response of an internally pressurized shell. To prevent this undesirable deformation, cross bars are mounted between the hinge points as shown in the figure such that the distance between the hinge points can be held constant or adjusted as needed to induce the appropriate stress state in the test panel. A detailed description of the D-box test fixture is presented in Ref. 3.

Finite Element Model

The load introduction region that attaches the curved panel to the D-box test fixture and the support condition along the two straight edges of the panel significantly influence the stress state in a curved stiffened panel tested in a D-box test fixture. Appropriate boundary conditions must be imposed on the panel so that its response simulates the corresponding shell response for a given loading condition. Finite element analyses were conducted to study the load introduction region and support conditions of a curved panel as a cylindrical shell and as a curved panel in the D-box test fixture. The finite element models for a cylindrical shell and the D-box test fixture with a corresponding test panel were generated using PATRAN (Ref. 4), and linear and nonlinear structural analyses were performed using STAGS (STructural Analysis of General Shells) computer code (Ref. 5). The nonlinear analyses for the pressure and the combined pressure and axial load cases have been performed for the cylindrical shell case to understand nonlinear effects. The panel/D-box assembly analysis was performed to adjust the cross bar forces so that the panel in the D-box experiences a stress state that is comparable to a cylindrical shell for a given loading condition.

The cylindrical shell is modeled using 186 triangular plate elements and 18,696 quadrilateral plate elements and has 117,330 degrees-of-freedom. To simulate the cylindrical shell subjected to internal pressure, the curved panel for the D-box test fixture is analyzed with boundary conditions that only permit radial displacements along the straight edge. The cylindrical shell reference model is presented in Figure 5(a). The D-box test fixture assembly with the curved panel is modeled with 25,145 quadrilateral and 366 triangular plate elements, 852 bar and spring elements amounting to 154,716 degrees-of-freedom. The curved panel/D-box test fixture model consisted of 18,696 quadrilateral plate elements, 366 triangular elements, and 426 beam elements. The curved panel/D-box test fixture model is presented Figure 5(b).

Results and Discussion

The aluminum panel/D-box test fixture were analyzed for selected loading conditions to determine the panel response when subjected to internal pressure only, axial compression with and without pressure, and combined axial compression and shear with and without pressure. Analytical buckling load results for the curved panel/D-box assembly are summarized in Table 2 for selected loading conditions. Selected analytical results are compared with the experimental results in this section. The stabilizing and destabilizing effects of different loading components can be clearly seen here.

Combined 8.0 psi internal pressure and 976 lb/in. axial load

The analytical radial displacement contours for the panel in the D-box test fixture are compared with the reference shell results in Figure 6. The results indicate that the boundary effects in the D-box test fixture influence the radial displacement at the load introduction region in the axial direction as well as in the hoop direction. The displacements on the interior of the test panel compare well with the results from the reference shell model shown in Figure 6(a).

The hoop stress resultants in the cylindrical shell model are compared to the test results in Figure 7. The hoop stress resultant distribution in the cylindrical shell model (Fig. 7(a)) is uniform in the skin and frame regions. The maximum hoop stress resultant on the skin surface of 873 lb/in. occurs at the frame locations. The hoop stress resultants in the frame region where shear clips attach the frames to the skin are located is approximately 980 lb/in. The hoop stress resultant distribution for the corresponding state in the test panel in the D-box test fixtures with cross bars applying a compressive load to correct bending moments introduced by the D-box test fixture are shown in Figure 7(b). The compressive load applied by the 13 cross bars were determined by correlating the cylindrical shell and test results and are presented in Table 3. The maximum hoop stress resultant on the skin surface of 909 lb/in. occurs at the frame location; the hoop stress resultants of the frame region where shear clips that attach the frames to the skin are located is approximately 1,074 lb/in. The results presented in Figure 7 indicate that the D-box test fixture analytical results compare well with the analytical results obtained from a cylindrical shell analysis.

The curved panel/D-box assembly was subjected next to various combinations of combined axial, torsion, and pressure loading. The experimental strain results measured in the panel at locations shown in Figure 8, along Line A and Line B, will be presented for selected loading conditions. A comparison of experimental and analytical strain results along Line B for the curved panel subjected to a combined 976 lb/in axial load and 8 psi internal pressure loading are presented in Figure 9. The circular symbols represents hoop surface strain results taken from strain gages on the outer skin surface of the panel. The square symbols represents hoop surface strain results taken from strain gages on the inner surface of the skin. The solid and dashed lines represent analytical results for outer and inner surfaces, respectively, for the test panel. The results indicate that good agreement was obtained between the experimental and analytical results. The results also indicate that the hoop strain distribution is influenced by the frames that are attached to the skin.

Axial compression loading

Axial surface strain results for the curved panel subjected to axial compression loading are presented in Figure 10. Surface strain results taken from a back-to-back strain gage pairs located on the skin of the panel between stringers and frames as a function of applied axial load are presented in Figure 10. The open symbols represent experimental axial strain measurements taken from back-to-back strain gages located on the skin of the panel midway between adjacent stringers and frames. The filled symbol indicates the bifurcation buckling load calculated from the finite element analysis. The results indicate that the panel buckled at approximately -158 kips axial load which compares well with the analytical buckling calculation of -165 kips.

Experimental axial strain results along Line A are presented in Figure 11(a) for the curved panel subjected to axial compression load. The strain results for applied axial loads of -35.2, -105.5, and -165.1 kips are presented in this figures 11(a). The strain results for applied axial loads of -34.6, -104.7, and -162.3 kips with 8.1 psi internal pressure loading are presented in Figure 11(b). The open and filled symbols indicate axial surface strain results taken from strain gages located on the outer and inner surfaces of the panel, respectively. The solid and dashed lines represent outer surface and inner surface analytical results respectively, from the finite element analysis of the curved panel/D-box assembly. The strain results suggest that the axial strain distribution was uniform across the panel.

Torsion loading

Surface strain results taken from a back-to-back strain gage pair located on the skin of the panel between stringers and frames as a function of applied torsion are presented in Figure 12. The open symbols represent experimental axial strain measurements taken from back-to-back strain gages located on the skin of the panel midway between the adjacent stringers and frames. The filled symbol indicates the bifurcation buckling load calculated from the finite element analysis. The circular symbols represent results for the curved panel/D-box assembly subjected to torsion loading. The square symbols represent results for the curved panel/D-box assembly subjected to torsion loading and 8 psi internal pressure loading. The results indicate that the panel buckled at about 6,883 in.-kips applied torsion for the panel subjected to torsion loading only and 11,525.4 in.-kips for the curved panel/D-box assembly subjected to combined torsion and 8 psi internal pressure loading. The analytical buckling calculations indicate that the buckling load was increased by 40% when

the curved panel/D-box assembly was subjected to combined torsion loading and 8 psi internal pressure loading. The experimental results compare well with the analytical bifurcation buckling load calculated from the finite element analysis.

Experimental shear strain results along Line A are presented in Figure 13 for the curved panel subjected to applied torsion loading and 8 psi internal pressure load. The open symbol indicates surface shear strain results for an applied torsion load of 5,501 in.-kips. The filled symbols indicates results for an applied torsion load of 5,521.1 in.-kips and 10,512 in.-kips with 8.1 psi internal pressure loading. The solid and dashed lines indicate surface strain results taken from strain gages located on the outer and inner surface of the panel, respectively. The strain results presented in this figure for 5,521.1 in.-kips and 8.1 psi internal pressure loading are uniform across the panel. However, the strain results presented in the figure for 5,501 in.-kips torsion load and no internal pressure suggest local bending in the skin of the panel between stringers as indicated by a difference in results taken from back-to-back strain gage pairs. The strain results presented in the figure for combined 10,512 in.-kips and 8.1 psi internal pressure loading suggest local bending in the skin of the panel as indicated by the difference in results taken from back-to-back strain gage pairs located between stringers.

Axial compression and torsion loading

Surface strain results for the curved panel/D-box assembly subjected to axial compression and torsion without pressure as a function of applied compression are presented in Figure 14. Experimental axial strain measurements taken from back-to-back strain gages located on the skin of the panel midway between the adjacent stringers and frames are represented by the open symbols. The bifurcation buckling load calculated from the curved panel/D-box assembly finite element analysis is represented by the filled symbol. The analytical results indicate that the panel buckled at a combined load of -100 kips axial compression and 3,334 in.-kips applied torsion. The experimental results presented in Figure 14 compare well with the analytical bifurcation buckling load calculated from the finite element analysis.

Experimental strain results along Line A are presented in Figure 15 for the curved panel/D-box subjected to combined axial compression and torsion loading. The open circle indicates surface axial strain results for combined mechanical load of 25 kips axial compression and a torsion load of 1,347 in.-kips. The open square indicates surface strain results for combined mechanical load of 92.5 kips axial compression and a torsion load of 3,084 in.-kips. Surface strain results taken from strain gages located on the outer and inner surface of the panel are indicated by the solid and dashed lines, respectively. The strain results for 92.5 kips axial compression and a torsion load of 3,084 in.-kips. suggest local bending in the skin of the panel between stringers as indicated by divergence of results taken from back-to-back strain gage pairs.

A comparison of axial and hoop stress resultant contour results for a curved panel subjected to 162.8 kips axial compression load, 1109.5 in.-kips torsion, and 8.0 psi internal pressure loading are presented in Figure 16. The axial stress resultant contours are present in Figure 16(a). The maximum axial stress resultant on the skin surface of -877 lb/in. occurs where the stringers are attached to the skin. A maximum axial stress resultant of -1,400 lb/in. occurs in a region where two aluminum sheets were mechanically fastened and reinforced with a stringer. The region of the skin between stringers had a maximum axial stress resultant of -336 lb/in. The hoop stress resultant distribution for the corresponding state in the curved panel in the D-box test fixtures with cross bars applying a compressive load to correct bending moments introduced by the D-box test fixture are shown in Fig. 16(b). A maximum hoop stress resultant of 992 lb/in. occurs on the skin surface at the frame location. The hoop stress resultants of the frame region where shear clips attach the frames to the skin are located is approximately 1,432 lb/in.

Concluding Remarks

An experimental and analytical investigation has been conducted to study the structural response of a curved stiffened panel subjected to combined mechanical and internal pressure loads. Analytical results for the curved aluminum panel in the D-box test fixture indicate that the radial displacement was influenced by the load introduction effects of the D-box when compared with analytical results obtained for the reference shell model. However, displacement and stress resultant for the curved panel in the D-box test fixture compared well with results for the reference shell model.

Surface strain results indicate that the experimental buckling loads compare well with analytical results for the loading cases that were considered. A comparison of surface strain data from back-to-back strain gages located on the skin suggest that buckling occurred when the panel was subjected to combined mechanical loads with and without internal pressure, with combinations of loading components significantly influencing the buckling loads. The experimental and analytical buckling results indicate that the buckling load of the curved stiffened panel was influenced by the internal pressure loading when the panel was subjected to combined mechanical loads.

References

1 Mahler, M., Ley, R., Shah, C., Lin, W., and Rouse, M., "Propagation and Control of Crack-Like Damage in Curved Composite Panels Under Combined Loads," 41st AIAA/ASME/ASCE/AHS/ASC Structures, Structural Dynamics, and Materials Conference & Exhibit, AIAA-2000-1533, April 3-6, 2000.

2 Ambur, D. A., Rouse, M., Starnes, J.H., and Shuart, M. J., "Facilities for Combined Loads Testing of Aircraft Structures to Satisfy Structural Technology Development Requirements," presented at the 5th Annual Advanced Composites Technology Conference, Seattle, WA, August 22-36, 1994.

3. Ambur, D. R., Cerro, J. A., and Dickson, J. D., "D-Box Fixture for Testing Stiffened Panels in Compression and Pressure," Journal of Aircraft, Vol. 32, No. 6, Nov.-Dec. 1995, pp. 1382-1389.

4. Anon., PATRAN Plus User Manual - Release 3.0, PDA Engineering, Publication Number 2191023, September 1989.

5. Rankin, C. C., Brogan, F. A., Loden, W. A., and Cabiness, H. K., "STAGS Users Manual," Version 3.0, Lockheed Martin Missiles & Space Co., Inc., Advanced Technology Center, Report LMSC P032594, 2001.

Table 1. Typical material properties

	2024-T3 Aluminum	7075 Aluminum
Young's Modulus (Msi)	10.6	10.4
Shear Modulus (Msi)	4.0	3.9
Poisson's ratio	0.33	0.33

Table 2. Summary of analytical buckling load results

Axial Load, kips	Torsion, in.-kips	Pressure, psi.
165.14	0.0	0.0
314.94	0.0	8.0
0.0	6,883	0.0
0.0	8,709.2	5.0
0.0	11,525.4	8.0
-100.0	3,334.0	0.0
-200.0	5,886.0	5.0
-200.0	9,027.6	8.0

Table 3. Calculated cross bar forces for test panel subjected to 8 psi. internal pressure

Cross brace actuator	Force, lb.
1	16,000
2	22,400
3	11,200
4	8,800
5	9,920
6	9,920
7	9,600
8	10,240
9	9,600
10	9,600
11	16,000
12	20,800
13	16,000

a. Photograph of test panel

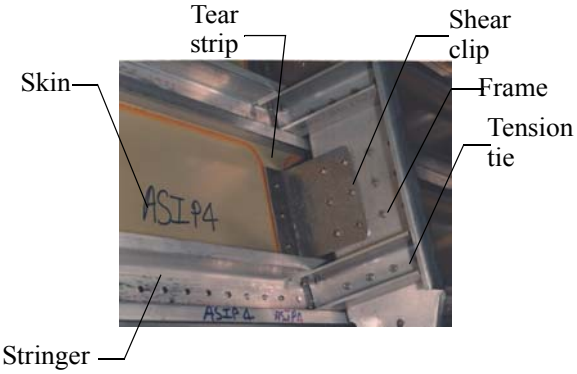

b. Structural details of aluminum pane

Figure 1. Description of test specimen.

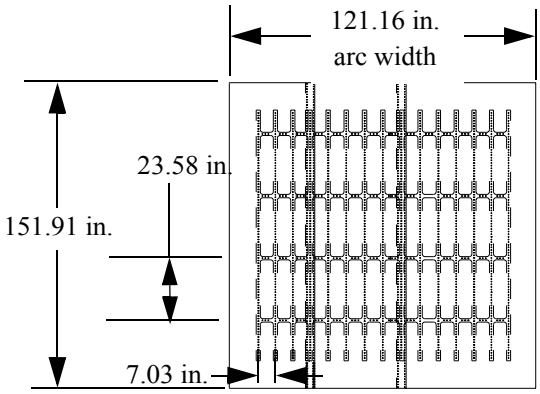

a. Panel geometry

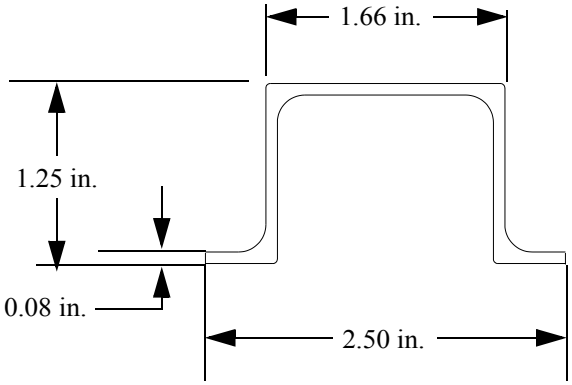

b. Stringer dimensions

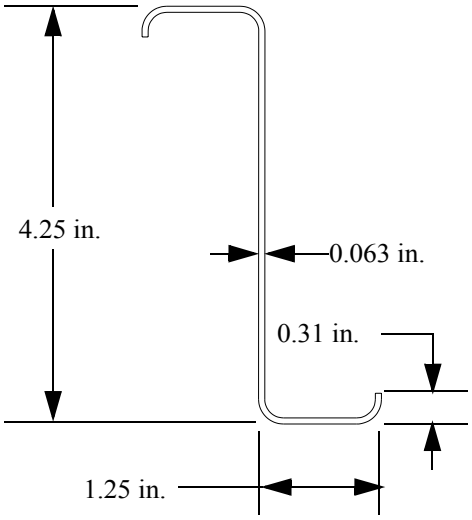

c. Frame dimensions

Figure 2. Continued

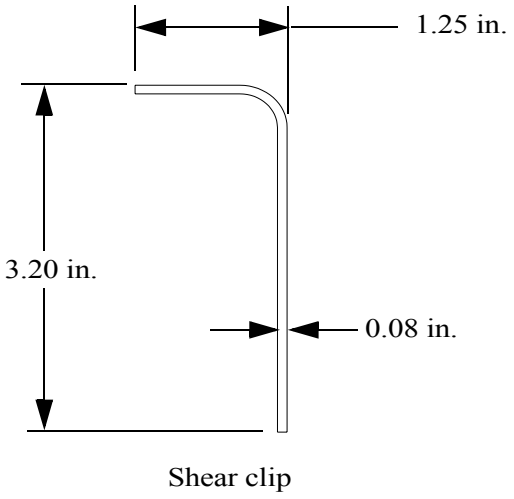

d. Shear clip dimensions

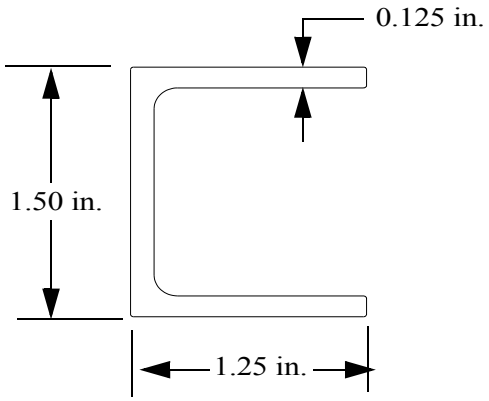

e. Tension tie dimensions

Figure 2. Panel geometry, stringer, and frame details.

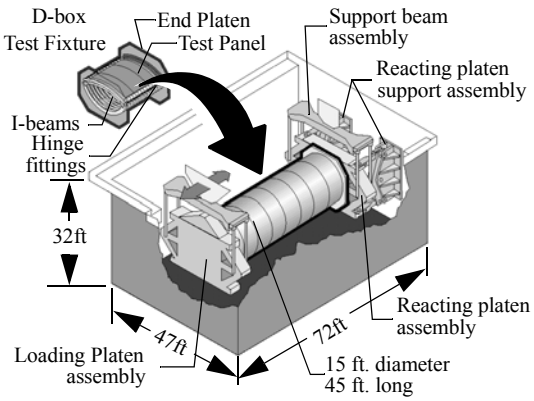

Figure 3. NASA Combined loads test machine.

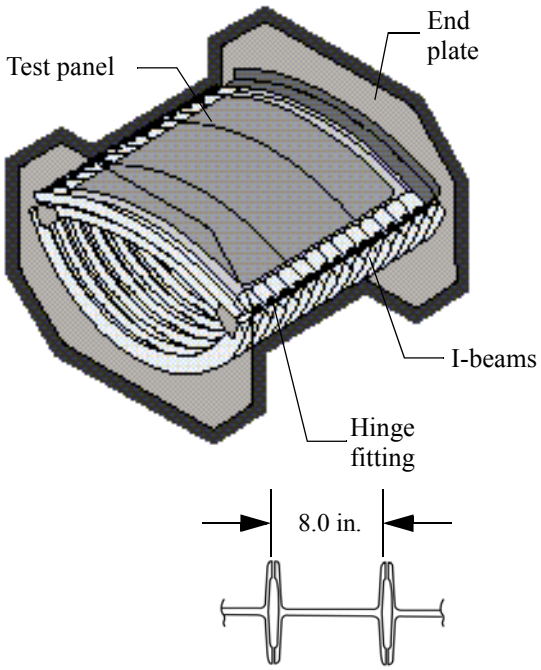

a. Overall configuration

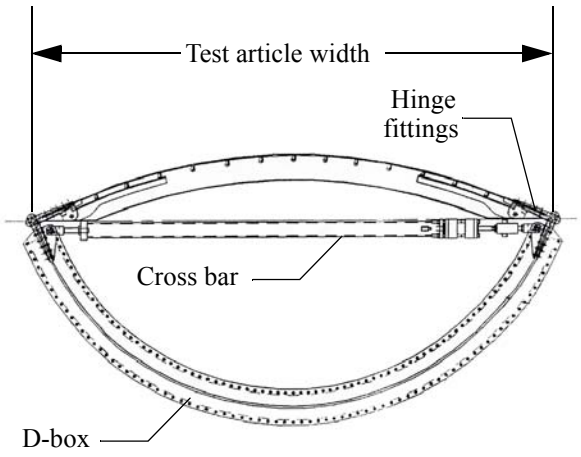

b. Cross-sectional view

Figure 4. D-box test fixture for testing curved stiffened panels.

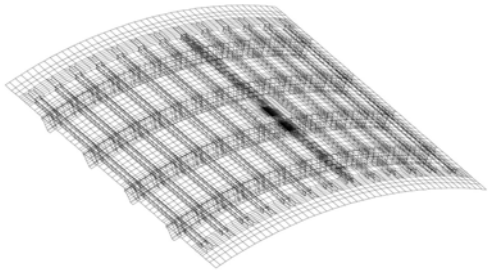

a. Cylindrical shell reference model

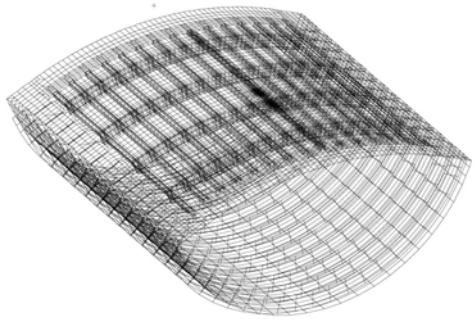

b. Curved panel/D-box assembly

Figure 5. Description of finite element models.

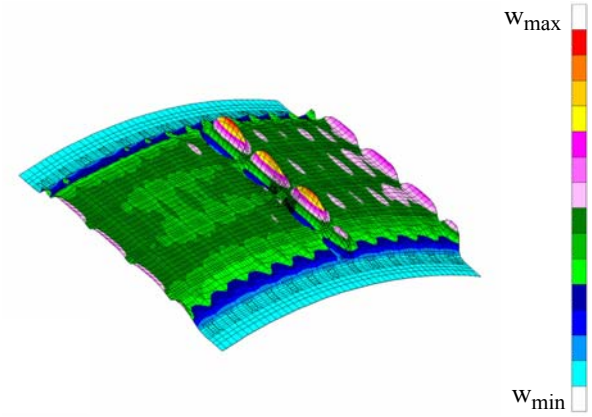

a. Cylindrical shell model

Figure 6. Continued.

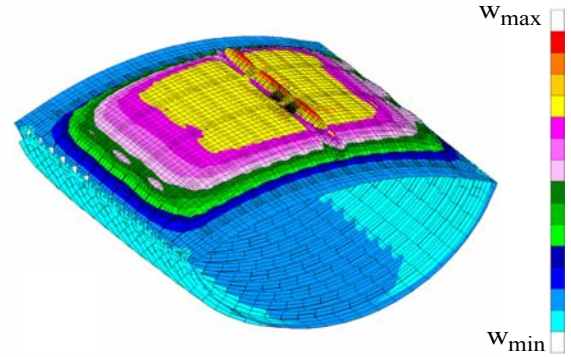

b. Panel in D-box test fixture

Figure 6. Analytical radial displacement contours for reference shell model and curved panel in D-box test fixture subjected to combined 8 psi internal loading and 976 lb/in. axial load.

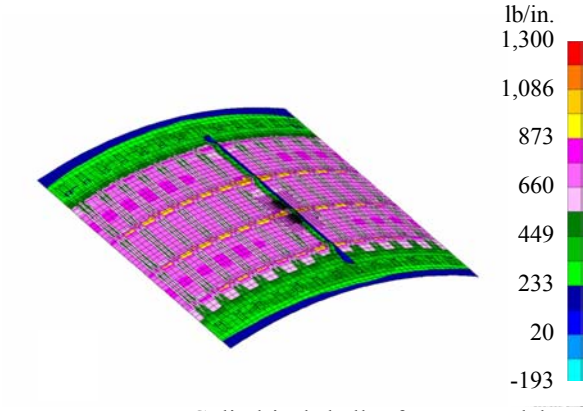

a. Cylindrical shell reference model

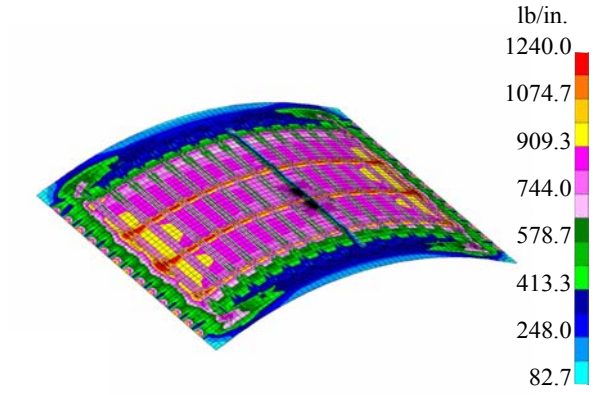

b. Curved panel in D-box test fixture.

Figure 7. Analytical hoop stress resultant contours for the reference shell model and curved panel in the D-box test fixture subject to 8 psi internal loading and 976 lb/in.

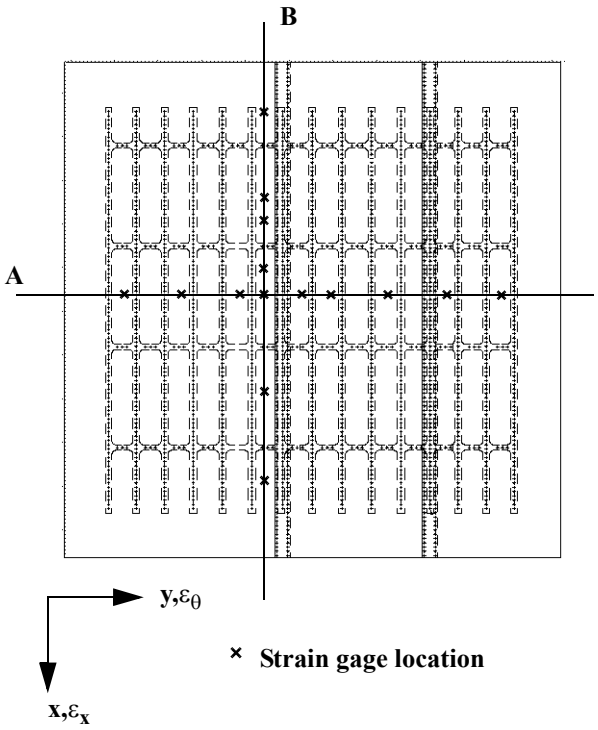

Figure 8. Location of selected strain gages on the skin surface of the panel.

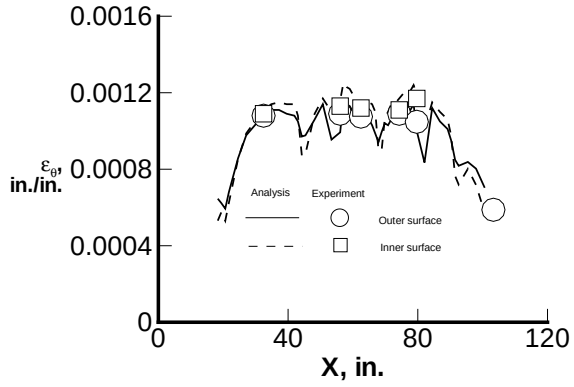

Figure 9. Comparison of experimental and analytical strain results along Line B for the curved panel in the D-box test fixture subjected to 8 psi internal pressure loading.

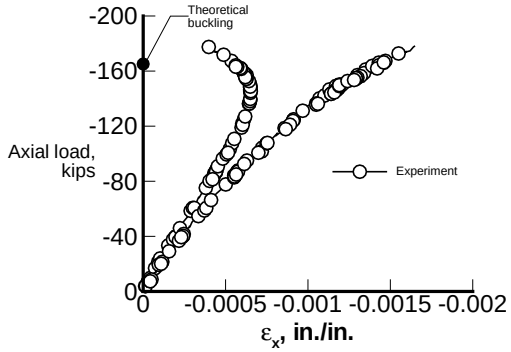

Figure 10. Back-to-back surface strain results as a function of applied axial load for a curved panel subjected to axial compression load.

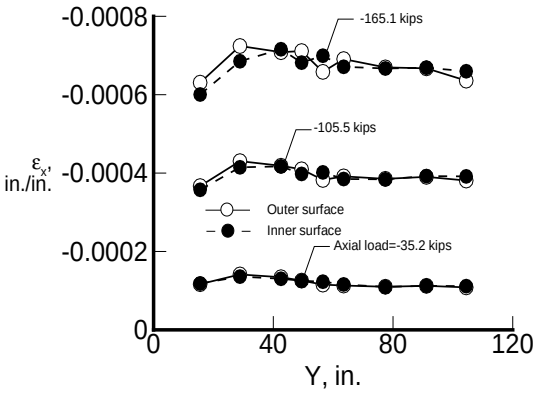

a. Axial load only

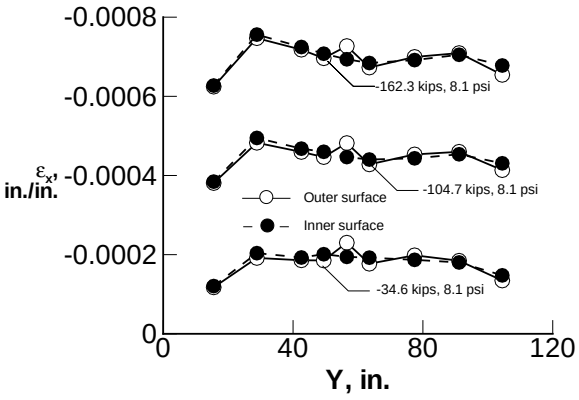

b. Combined axial load and 8 psi internal pressure loading

Figure 11. Experimental axial surface strain results from back-to-back strain gages along Line A for a curved panel subjected to axial compression load with and without 8 psi internal pressure loading.

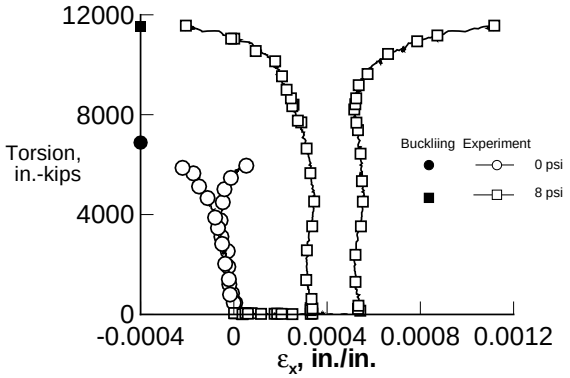

Figure 12. Experimental or axial surface strains results from back-to-back strain gages as a function of applied torsion load with and without 8 psi internal pressure loading.

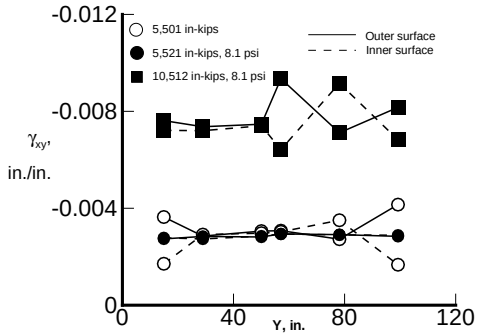

Figure 13. Experimental surface strains from back-to-back strain gages along Line A for a curved panel subjected to torsion loading with and without 8 psi internal pressure loading.

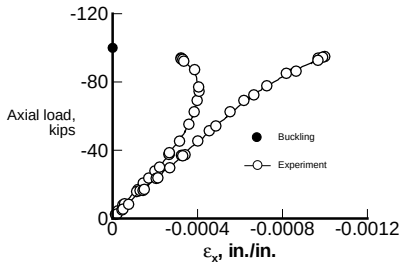

Figure 14. Experimental surface axial strains from back-to-back strain gages for a curved panel subjected to axial compression and torsion loading.

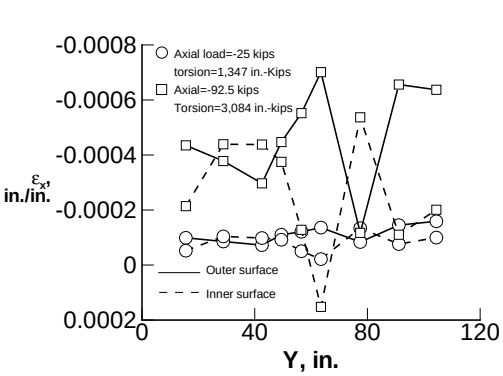

Figure 15. Experimental surface axial strains from back-to-back strain gages along Line A for a curved panel subjected to axial compression and torsion loading.

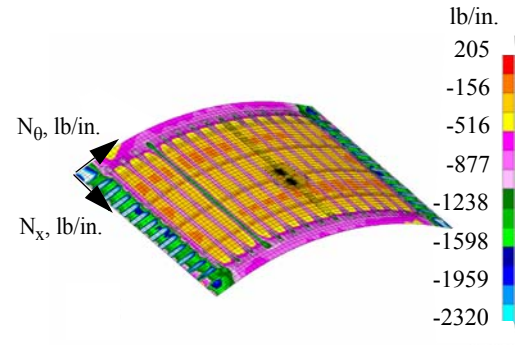

a. Resultant axial stress (N_x) contours

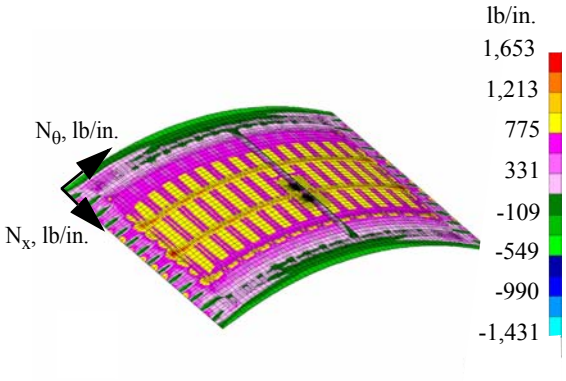

b. Resultant hoop stress (N_θ) contours

Figure 16. Comparison of stress resultant contours for a curved panel subjected to combined axial, torsion and internal pressure loading.